*Inorg. Chem.* **2004**, *43*, 8414–8426


# Metal Carbonyl Derivatives of Sulfur-Containing Quinones and Hydroquinones: Synthesis, Structures, and Electrochemical Properties

**Richard D. Adams* and Shaobin Miao**

*Department of Chemistry and Biochemistry, University of South Carolina, Columbia, South Carolina 29208*

Received August 15, 2004

The reaction of $CpMoMn(\mu\text{-}S_2)(CO)_5$, **1**, with 1,4-benzoquinone in the presence of irradiation with visible light yielded the quinonedithiolato complex $CpMoMn(CO)_5(\mu\text{-}S_2C_6H_2O_2)$, **2**. The new complex $CpMoMn(CO)_5(\mu\text{-}S_2C_6Cl_2O_2)$ (**4**) was synthesized similarly from **1** and 2,3-dichloro-1,4-benzoquinone. Compounds **2** and **4** were reduced with hydrogen to yield the hydroquinone complexes $CpMoMn(CO)_5[\mu\text{-}S_2C_6H_2(OH)_2]$, **3**, and $CpMoMn(CO)_5[\mu\text{-}S_2C_6Cl_2(OH)_2]$, **5**. UV–vis irradiation of solutions of $Fe_2(CO)_6(\mu\text{-}S_2)$ and 1,4-benzoquinone yielded the hydroquinone complex $Fe_2(CO)_6[\mu\text{-}S_2C_6H_2(OH)_2]$, **6**. Compound **6** was oxidized to the quinone complex $Fe_2(CO)_6(\mu\text{-}S_2C_6H_2O_2)$, **7,** by using 2,3-dichloro-5,6-dicyano-1,4-benzoquinone. Substitution of the CO ligands on **6** by $PPh_3$ yielded the derivatives $Fe_2(CO)_5(PPh_3)[\mu\text{-}S_2C_6H_2(OH)_2]$, **8**, and $Fe_2(CO)_4(PPh_3)_2[\mu\text{-}S_2C_6H_2(OH)_2]$, **9**. The electrochemical properties of **3**, **5**, **6**, **8**, and **9** were measured by cyclic voltammetry. The molecular structure of each of the new compounds **2**–**9** was established by single-crystal X-ray diffraction analyses.

## Introduction

Metal complexes containing disulfido ligands have been attracting considerable attention because of their involvement in important biological processes.[1] Disulfido ligands engage in a wide variety of bridging coordination geometries.[2] In dinuclear metal complexes disulfido and diselenido ligands are known to react with unsaturated organic molecules by insertion into the S−S and Se−Se bonds.[3] We have recently synthesized the mixed-metal disulfido complex, $CpMoMn(CO)_5(\mu\text{-}S_2)$, **1**[4] and have studied the insertion of metal groups and unsaturated molecules ranging from CO and olefins to dienes and even $C_{60}$ into its S−S bond, eq 1[5] and eq 2.[4,6] It has been shown that the insertion of unsaturated molecules into the S−S bond of the disulfido ligand in these dimetal complexes is promoted by UV−vis irradiation.[3d−3f,6,7] Mechanistic studies are consistent with a "concerted" addition process, which is similar to that of the classic [2+2] cycloaddition reaction of organic compounds which is thermally symmetry forbidden but photochemically allowed.[8]

Quinones are effective bridging ligands and have been used to form extensive supramolecular coordination networks.[9] Quinones are also very important bioactive molecules that contain C−C double bond. Quinone derivatives play important roles in biological processes such as cellular respiration,[10] photosynthesis[11] and blood coagulation.[12] Their biological action is often linked to their electron-transfer rates

* To whom correspondence should be addressed. E-mail: adams@mail.chem.sc.edu.

(1) (a) Malinak, S. M.; Coucouvanis, D. *Prog. Inorg. Chem.* **2001**, *49*, 599. (b) Holm, R. H. *Pure Appl. Chem.* **1998**, *70*, 931. (c) Beinert, H.; Holm, R. H.; Munck, E. *Science* **1997**, *277*, 653. (d) Holm, R. H. *Adv. Inorg. Chem.* **1992**, *38*, 1. (e) Shibahara, T. *Coord. Chem. Rev.* **1993**, *123*, 73. (f) Coucouvanis, D. *Acc. Chem. Res.* **1991**, *24*, 1. (g) Lindahl, P. A.; Kovacs, J. A. *J. Cluster Sci.* **1990**, *1*, 29. (h) Burgess, B. K. *Chem. Rev.* **1990**, *90*, 1377.

(2) (a) Müller, A.; Jaegermann, W.; Enemark, J. H. *Coord. Chem Rev.* **1982**, *46*, 245. (b) Matsumoto, K.; Koyama, T.; Furuhashi, T. *ACS Sym. Ser.* **1996**, *653*, 251.

(3) (a) King, R. B.; Bitterwolf, T. E. *Coord. Chem. Rev.* **2000**, *206*−*207*, 563. (b) Whitmire, K. H. In *Comprehensive Organometallic Chemistry II*; Wilkinson, G., Stone, F. G. A., Abel, E., Eds.; Pergamon Press: New York, 1995; Vol. 7, Chapter 1, Section 1.11.2.2, p 62, and references therein. (c) Mathur, P. *Adv. Organomet. Chem.* **1997**, *41*, 243. (d) Kramer, A.; Lingnau, R.; Lorenz, I.-P.; Mayer, H. A. *Chem. Ber.* **1990**, *123*, 1821. (e) Messelhäuser, J.; Gutensohn, K. U.; Lorenz, I.-P.; Hiller, W. *J. Organomet. Chem.* **1987**, *321*, 377. (f) Messelhäuser, J.; Lorenz, I.-P.; Haug, K.; Hiller, W. Z. *Naturforsch.* **1985**, *40B*, 1064. (g) Adams, R. D.; Kwon, O. S. *Inorg. Chem.* **2003**, *42*, 6175.

(4) Adams, R. D.; Captian, B.; Kwon, O.; Miao, S. *Inorg. Chem.* **2003**, *42*, 3356.

(5) Adams, R. D.; Miao, S. *Organometallics* **2003**, *22*, 2492.

(6) Adams, R. D.; Miao, S.; Smith, M. D. *Organometallics* **2004**, *23*, 3327.

(7) Kramer, A.; Lorenz, I.-P. *J. Organomet. Chem.* **1990**, *388*, 187.

(8) Woodward, R. B.; Hoffmann, R. *The Conservation of Orbital Symmetry*; Verlag Chemie, Weinheim, Germany, 1989.

(9) Oh, M.; Carpenter, G. B.; Sweigart, D. A. *Acc. Chem. Res.* **2004**, *37*, 1.

(10) (a) Larsen, P. L.; Clarke, C. F. *Science* **2002**, *295*, 120. (b) Do, T. Q.; Hsu, A. Y.; Jonassen, T.; Lee, P. T.; Clarke, C. F. *J. Biol. Chem.* **2001**, *276*, 18161.



10.1021/ic048880w CCC: $27.50 
Published on Web 11/25/2004

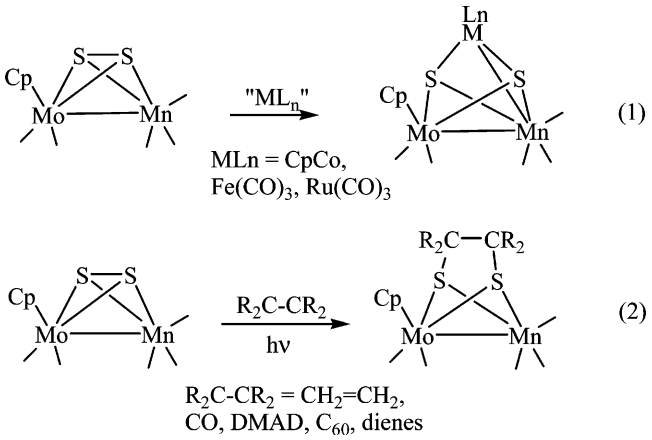


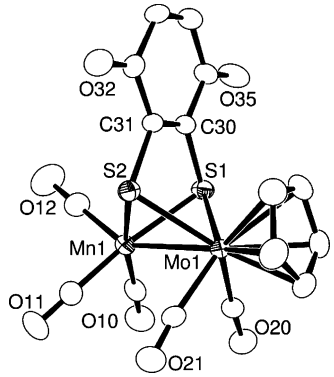


**Figure 1.** ORTEP diagram of the molecular structure of **2**, showing 40% thermal ellipsoid probability.

and redox potentials.[13] In organic synthesis, quinones are valuable reagents for the dehydrogenation of polycyclic hydroaromatic compounds,[14] alcohols,[15] cyclic ketones and nitrogen heterocycles.[16] Quinone/hydroquinone redox couples have been widely used in electrochemical studies because they are readily available and exhibit "well behaved" electrochemistry.

We have now prepared some metal carbonyl derivatives of sulfur-containing quinones and hydroquinones by the photopromoted reaction of quinones with **1** and $Fe_2(CO)_6(\mu\text{-}S_2)$ and have investigated their structures and electrochemical properties. These results are reported here. A preliminary report of this work has been published.[17]

## Results and Discussion

The reaction of **1** with 1,4-benzoquinone in the presence of irradiation from a tungsten lamp afforded the quinone derivative, $CpMoMn(CO)_5(\mu\text{-}S_2C_6H_2O_2)$, **2**, in 67% yield. The reaction does not proceed in the absence of light.[6,7] The infrared spectrum of **2** exhibits four absorptions between 2035 and 1931 $cm^{-1}$ that can be attributed to terminal carbonyl ligands and one peak at 1651 $cm^{-1}$ which can be assigned to ketone groups of 1,4-benzoquinone grouping. The $^1H$ NMR spectrum of **2** shows two singlets at 6.62 and 5.98 ppm that can be assigned to the olefinic and Cp ring protons, respectively. Details of molecular structure of **2** were established by a single-crystal X-ray diffraction analysis, and an ORTEP diagram of its molecular structure is shown in Figure 1. Selected bond distances and angles are listed in Table 1.

The structure of **2** is similar to that of **1** except that there is a 1,4-quinone-2,3-dithiolato ligand that bridges two metal atoms in the place of the disulfido ligand in **1**. The manganese atom and molybdenum atom are joined by a metal−metal single bond. The Mn−Mo bond distance in **2**, 2.7050(6) Å, is shorter than that found in **1**, 2.8421(10) Å.[4] The S(1)···S(2) distance, 3.042 (3) Å, is nonbonding, and is even longer than the S···S distance, 2.959(4) Å, found in the related ethanedithiolate compound $CpMoMn(CO)_5(\mu\text{-}SCH_2CH_2S)$.[4] The C−O bond lengths in the quinone group are typical of C−O double bonds, 1.221(4) Å and 1.218(5) Å. Two of C−C bonds in the six-membered ring, C(30)−C(31) = 1.338(5) Å and C(33)−C(34) = 1.316(6) Å, are short and double in character as expected. These are not significantly different from those found in 1,4-benzoquinone itself, 1.334(3) Å.[18] The other C−C bonds are much longer and single in character, 1.474(4)−1.476(5) Å.

Two of the hydrogen atoms on the 1,4-benzoquinone molecule were replaced with the sulfur atoms of **1** to form the 2,3-dithiolato-1,4-benzoquinone ligand. In the process the S−S bond in **1** was cleaved. The yield of **2** is increased in the presence of an excess of 1,4-quinone and 1,4-hydroquinone is a coproduct. It is proposed that the reaction proceeds first by an insertion of one of the C−C double bonds of the benzoquinone into the S−S bond of **1**, as previously observed for olefins,[6] and is followed by an oxidative cleavage of the two hydrogen atoms from those two carbon atoms by a second equivalent of 1,4-benzoquinone, Scheme 1.

Treatment of **2** with hydrogen in the presence of light provided the reduced complex $CpMoMn(CO)_5[\mu\text{-}S_2C_6H_2(OH)_2]$, **3**, in 86% yield, Scheme 1. Compound **3** was characterized by a combination of IR, $^1H$ NMR and single-crystal X-ray diffraction analysis. The infrared spectrum of **3** is very similar to that of **2**, but the lower frequency absorptions of the C═O functions of the quinone group are no longer present. The $^1H$ NMR spectrum of **3** shows three singlets at 6.22, 5.68, and 4.82 ppm which are assigned to protons on the hydroquinone ring, the Cp ring and the OH groups, respectively. The molecular structure of **3** was established by a single-crystal X-ray diffraction analysis, and an ORTEP diagram of its molecular structure is shown in Figure 2. Selected bond distances and angles are listed in

(11) Steinberg-Yfrach, G.; Liddell, P. A.; Hung, S.-C.; Moore, A. L.; Gust, D.; Moore, T. A. *Nature* **1997**, *385*, 239.
(12) Cross, J. V.; Deak, J. C.; Rich, E. A.; Qian, Y.; Lewis, M.; Parrott, L. A.; Mochida, K.; Gustafson, D.; Vande Pol, S.; Templeton, D. J. *J. Biol. Chem.* **1999**, *274*, 31150.
(13) Voet, D.; Voet, J. B.; Pratt, C. W. *Fundamentals of Biochemistry*; Wiley: New York, 1999.
(14) Fu, P. P.; Harvey, R. G. *Chem. Rev.* **1978**, *78*, 317.
(15) Csjernyik, G.; Ell, A. H.; Fadini, L.; Pugin, B.; Bäckvall, J.-E., *J. Org. Chem.* **2002**, *67*, 1657.
(16) Becker, H.-D.; Turner, A. B. In *The Chemistry of Quinonoid Compounds*; Patai, S., Rappoport, Z., Eds.; Wiley: New York, 1988; Vol. 2, Chapter 23, pp 1351−1384.
(17) Adams, R. D.; Miao, S. *J. Am. Chem. Soc.* **2004**, *126*, 5056.
(18) Van Bolhuis, F.; Kiers, C. T. *Acta Crystallogr. B: Struct. Crystallogr. Cryst. Chem.* **1978**, *34*, 1015.

**Table 1.** Selected Intramolecular Bond Distances and Angles for **2**[a]

(a) Distances

| atom | atom | distance (Å) | atom | atom | distance (Å) |
|---|---|---|---|---|---|
| Mo(1) | S(1) | 2.4931(9) | O(35) | C(35) | 1.218(5) |
| Mo(1) | S(2) | 2.5096(9) | C(30) | C(31) | 1.338(5) |
| Mo(1) | Mn(1) | 2.7050(6) | C(30) | C(35) | 1.474(4) |
| Mn(1) | S(1) | 2.3557(9) | C(31) | C(32) | 1.474(5) |
| Mn(1) | S(2) | 2.3582(11) | C(32) | C(33) | 1.474(5) |
| S(1) | C(30) | 1.776(3) | C(33) | C(34) | 1.316(6) |
| S(2) | C(31) | 1.781(3) | C(34) | C(35) | 1.476(5) |
| O(32) | C(32) | 1.221(4) | C | O | 1.140(4) (av) |
| | | | S(1) | S(2) | 3.042(3) |

(b) Angles

| atom | atom | atom | angle (deg) | atom | atom | atom | angle (deg) |
|---|---|---|---|---|---|---|---|
| S(1) | Mo(1) | S(2) | 74.90(3) | C(31) | S(2) | Mo(1) | 98.86(11) |
| S(1) | Mo(1) | Mn(1) | 53.71(2) | Mn(1) | S(1) | Mo(1) | 67.75(3) |
| S(2) | Mo(1) | Mn(1) | 53.61(2) | C(31) | C(30) | C(35) | 121.5(3) |
| S(1) | Mn(1) | S(2) | 80.38(3) | C(31) | C(30) | S(1) | 118.9(2) |
| S(1) | Mn(1) | Mo(1) | 58.54(2) | Mn(1) | S(2) | Mo(1) | 67.43(3) |
| S(2) | Mn(1) | Mo(1) | 58.95(2) | C(35) | C(30) | S(1) | 119.6(3) |
| C(30) | S(1) | Mn(1) | 101.40(11) | C(30) | C(31) | C(32) | 121.7(3) |
| C(30) | S(1) | Mo(1) | 99.11(11) | C(30) | C(31) | S(2) | 118.4(2) |
| C(31) | S(2) | Mn(1) | 101.33(12) | C(32) | C(31) | S(2) | 119.9(3) |

[a] Estimated standard deviations in the least significant figure are given in parentheses.

**Scheme 1**

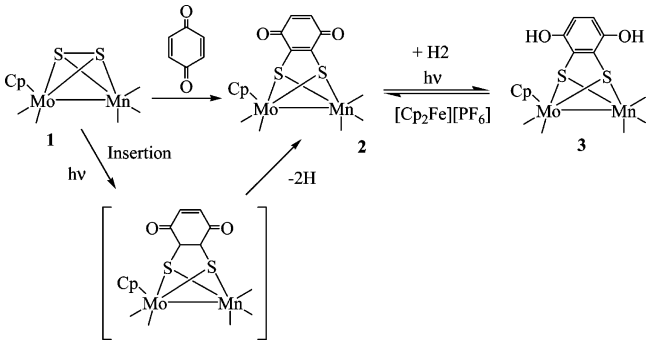


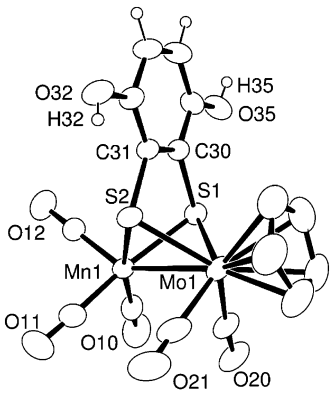


**Figure 2.** ORTEP diagram of the molecular structure of **3**, showing 40% thermal ellipsoid probability.

Table 2. The structure of **3** is similar to that of **2** except that the benzoquinone group has been reduced to a hydroquinone group. The Mn−Mo bond distance, 2.7418(3) Å, is longer than that in **2**, but still shorter than that in **1**. The sulfur atoms are not mutually bonded in **3**, S···S = 2.989(3) Å. The $C_6$ ring appears to be fully delocalized. The C−C distances in the ring span the narrow range: 1.375(2)−1.396(3) Å. As expected, one hydrogen atom was observed on each of the oxygen atoms, O(32) and O(35). The C−O bond distance, 1.363(2) Å and 1.366(2) Å, is typical of C−O single bonds. In the solid state the molecules of the complex are arranged in zigzag chains that run parallel to the *c*-axis and are linked by hydrogen bonds between the hydroxyl groups of the hydroquinone functions and to a molecule of diethyl ether that cocrystallized with the complex, see Figure 3.

Compound **3** was reoxidized to **2** in 84% yield by treatment with ferrocenium hexafluorophosphate. The electrochemical properties of **3** were measured by cyclic voltammetry (CV) in acetonitrile by using the tetrabutylammonium hexafluorophosphate as the supporting electrolyte. The cyclic voltammograms of **3** are shown in Figure 4. Two redox couples were observed at −0.34, −1.0 V versus Ag/AgCl. These redox couples are quasi-reversible.

The reaction of $CpMoMn(CO)_5(\mu\text{-}S_2)$ with 2,3-dichloro-1,4-benzoquinone afforded the new compound, $CpMoMn(CO)_5(\mu\text{-}S_2C_6Cl_2O_2)$, **4**, in 38% yield, Scheme 2. The molecular structure of **4** was determined by single-crystal X-ray diffraction analysis, and an ORTEP diagram of its molecular structure is shown in Figure 5. Selected bond distances and angles are listed in Table 3. The molecular structure of **4** is similar to that of **2** except for a 2,3-dichlorobenzoquinone group in the place of the 1,4-benzoquinone group. The Mo−Mn bond distance, 2.7288(6) Å [2.7186(6) Å], is slightly longer than that in **2**, but still shorter than that in **1**. The bond distances in 2,3-dichlorobenzoquinone group are as expected for this quinone group.

Reduction of compound **4** by hydrogen provided the compound **5**, $CpMoMn(CO)_5[\mu\text{-}S_2C_6Cl_2(OH)_2]$ in 83% yield. Details of molecular structure of **5** were established by a single-crystal X-ray diffraction analysis, and an ORTEP diagram of its molecular structure is shown in Figure 6. Selected bond distances and angles are listed in Table 4. Its

**Table 2.** Selected Intramolecular Bond Distances and Angles for **3**[a]

(a) Distances

| atom | atom | distance (Å) | atom | atom | distance (Å) |
|---|---|---|---|---|---|
| Mo(1) | S(1) | 2.4824(5) | O(35) | C(35) | 1.366(2) |
| Mo(1) | S(2) | 2.4851(5) | C(30) | C(31) | 1.390(2) |
| Mo(1) | Mn(1) | 2.7418(3) | C(30) | C(35) | 1.375(2) |
| Mn(1) | S(1) | 2.3236(5) | C(31) | C(32) | 1.385(2) |
| Mn(1) | S(2) | 2.3341(5) | C(32) | C(33) | 1.393(3) |
| S(1) | C(30) | 1.7866(17) | C(33) | C(34) | 1.377(3) |
| S(2) | C(31) | 1.7826(17) | C(34) | C(35) | 1.396(3) |
| O(32) | C(32) | 1.363(2) | C | O | 1.141(3) (av) |
| | | | S(1) | S(2) | 2.989(3) |

(b) Angles

| atom | atom | atom | angle (deg) | atom | atom | atom | angle (deg) |
|---|---|---|---|---|---|---|---|
| S(1) | Mo(1) | S(2) | 73.998(15) | C(31) | S(2) | Mo(1) | 100.35(6) |
| S(1) | Mo(1) | Mn(1) | 52.532(13) | Mn(1) | S(1) | Mo(1) | 69.480(15) |
| S(2) | Mo(1) | Mn(1) | 52.767(13) | C(35) | C(30) | C(31) | 120.77(16) |
| S(1) | Mn(1) | S(2) | 79.856(18) | C(35) | C(30) | S(1) | 122.45(13) |
| S(1) | Mn(1) | Mo(1) | 57.988(14) | Mn(1) | S(2) | Mo(1) | 69.272(14) |
| S(2) | Mn(1) | Mo(1) | 57.961(14) | C(31) | C(30) | S(1) | 116.78(13) |
| C(30) | S(1) | Mn(1) | 102.69(6) | C(32) | C(31) | C(30) | 120.66(16) |
| C(30) | S(1) | Mo(1) | 100.33(6) | C(32) | C(31) | S(2) | 122.88(13) |
| C(31) | S(2) | Mn(1) | 102.80(6) | C(30) | C(31) | S(2) | 116.46(12) |

[a] Estimated standard deviations in the least significant figure are given in parentheses.

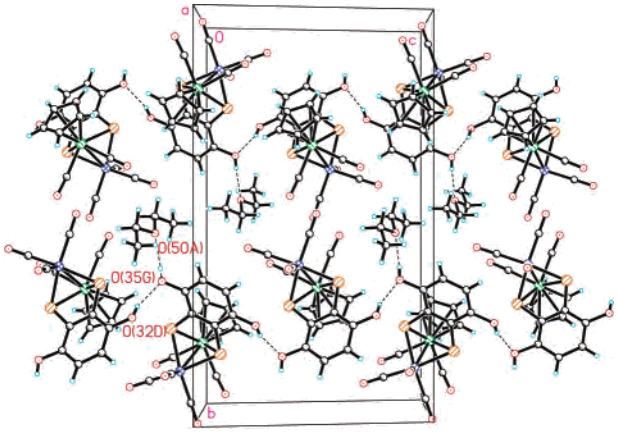


**Figure 3.** Packing diagram of the structure of **3** showing intermolecular hydrogen bonding between the hydroquinone groups and also with the cocrystallized diethyl ether.

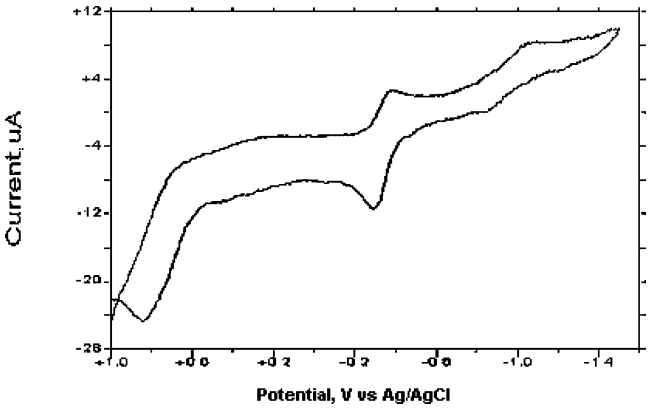


**Figure 4.** CV trace of **3** (1.0 mM) in $CH_3CN$ (10 mL) with 1.5 mM of $[Bu^n_4N]OH$ and 0.1 M of $[NBu^n_4]PF_6$ at scan rate 100 mV/Second.

molecular structure is similar to that of **4** except the $C_6$ ring is fully delocalized. One hydrogen atom is found on each of oxygen atoms, O(32) and O(35) and these appear in the $^1H$

**Scheme 2**

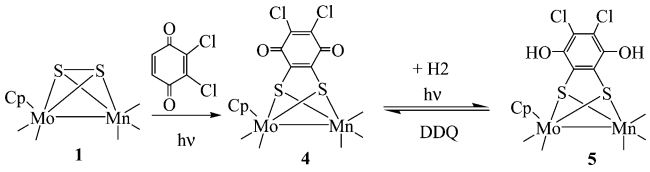


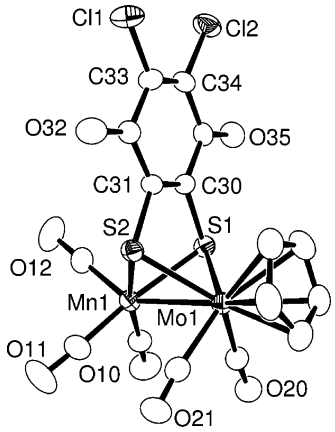


**Figure 5.** ORTEP diagram of the molecular structure of **4** showing 40% thermal ellipsoid probability.

NMR spectrum at 5.41 ppm. A CV trace of **5** is shown in Figure 7. The CVs of basic solutions of **5** in acetonitrile show two quasi-reversible one-electron redox processes: one at $E_{1/2} = -0.11$ V and a second at approximately $E_{1/2} = -0.9$ V. Compared to CV trace of $CpMoMn(CO)_5[\mu\text{-}S_2C_6H_2(OH)_2]$ in basic solution, the CV of **5** shows that **4** is a stronger oxidant than **2** as expected because of the presence of the two chlorine atoms on the quinone ring.

The reaction of $Fe_2(CO)_6(\mu\text{-}S_2)$ with 1,4-benzoquinone under UV−vis irradiation yielded the hydroquinone derivative $Fe_2(CO)_6[\mu\text{-}S_2C_6H_2(OH)_2]$, **6**, in 53% yield, eq 3. The mechanism of formation of **6** is not known, and it is possible

**Table 3.** Selected Intramolecular Bond Distances and Angles for **4**[a]

(a) Distances

| atom | atom | distance (Å) | atom | atom | distance (Å) |
|---|---|---|---|---|---|
| Mo(1) | S(1) | 2.4943(9) | Mo(2) | S(3) | 2.4935(10) |
| Mo(1) | S(2) | 2.5043(10) | Mo(2) | S(4) | 2.4991(10) |
| Mo(1) | Mn(1) | 2.7288(6) | Mo(2) | Mn(2) | 2.7186(6) |
| Mn(1) | S(2) | 2.3482(11) | Mn(2) | S(4) | 2.3451(11) |
| Mn(1) | S(1) | 2.3491(11) | Mn(2) | S(3) | 2.3585(11) |
| S(1) | C(30) | 1.777(4) | S(3) | C(70) | 1.765(4) |
| S(2) | C(31) | 1.777(3) | S(4) | C(71) | 1.776(3) |
| Cl(1) | C(33) | 1.702(4) | Cl(3) | C(73) | 1.711(4) |
| Cl(2) | C(34) | 1.711(4) | Cl(4) | C(74) | 1.712(4) |
| O(32) | C(32) | 1.228(4) | O(72) | C(72) | 1.213(5) |
| O(35) | C(35) | 1.219(4) | O(75) | C(75) | 1.223(4) |
| C(30) | C(31) | 1.337(5) | C(70) | C(71) | 1.336(5) |
| C(30) | C(35) | 1.472(5) | C(70) | C(75) | 1.477(5) |
| C(31) | C(32) | 1.460(5) | C(71) | C(72) | 1.470(5) |
| C(32) | C(33) | 1.492(5) | C(72) | C(73) | 1.479(5) |
| C(33) | C(34) | 1.330(6) | C(73) | C(74) | 1.338(5) |
| C(34) | C(35) | 1.487(5) | C(74) | C(75) | 1.486(5) |
| C | O | 1.142(5)(av) | S(1) | S(2) | 3.045(5) |
| | | | S(3) | S(4) | 3.038(5) |

(b) Angles

| atom | atom | atom | angle (deg) | atom | atom | atom | angle (deg) |
|---|---|---|---|---|---|---|---|
| S(1) | Mo(1) | S(2) | 75.05(3) | S(3) | Mo(2) | S(4) | 74.95(3) |
| S(1) | Mo(1) | Mn(1) | 53.23(2) | S(3) | Mo(2) | Mn(2) | 53.60(3) |
| S(2) | Mo(1) | Mn(1) | 53.11(2) | S(4) | Mo(2) | Mn(2) | 53.21(3) |
| S(2) | Mn(1) | S(1) | 80.81(4) | S(4) | Mn(2) | S(3) | 80.46(4) |
| S(2) | Mn(1) | Mo(1) | 58.54(3) | S(4) | Mn(2) | Mo(2) | 58.59(3) |
| S(1) | Mn(1) | Mo(1) | 58.27(3) | S(3) | Mn(2) | Mo(2) | 58.32(3) |
| C(30) | S(1) | Mn(1) | 100.31(12) | C(70) | S(3) | Mn(2) | 99.74(12) |
| C(30) | S(1) | Mo(1) | 99.07(12) | C(70) | S(3) | Mo(2) | 99.88(12) |
| Mn(1) | S(1) | Mo(1) | 68.51(3) | Mn(2) | S(3) | Mo(2) | 68.09(3) |
| C(31) | S(2) | Mn(1) | 99.83(12) | C(71) | S(4) | Mn(2) | 99.77(12) |
| C(31) | S(2) | Mo(1) | 99.45(12) | C(71) | S(4) | Mo(2) | 100.34(12) |
| Mn(1) | S(2) | Mo(1) | 68.35(3) | Mn(2) | S(4) | Mo(2) | 68.19(3) |
| C(31) | C(30) | C(35) | 122.2(3) | C(71) | C(70) | C(75) | 121.3(3) |
| C(31) | C(30) | S(1) | 118.7(3) | C(71) | C(70) | S(3) | 119.3(3) |
| C(35) | C(30) | S(1) | 119.1(3) | C(75) | C(70) | S(3) | 119.4(3) |
| C(30) | C(31) | C(32) | 121.9(3) | C(70) | C(71) | C(72) | 122.7(3) |
| C(30) | C(31) | S(2) | 118.7(3) | C(70) | C(71) | S(4) | 118.1(3) |
| C(32) | C(31) | S(2) | 119.4(3) | C(72) | C(71) | S(4) | 119.0(3) |

[a] Estimated standard deviations in the least significant figure are given in parentheses.

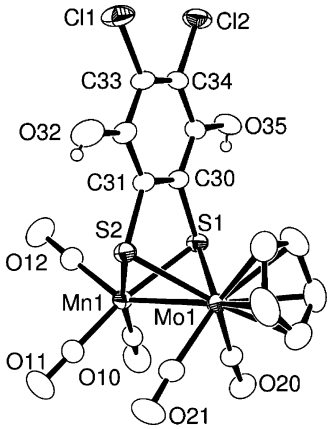


**Figure 6.** ORTEP diagram of the molecular structure of **5** showing 40% thermal ellipsoid probability.

that the reduction of the ketone groups was accomplished simply by intramolecular shift of the two hydrogen atoms from the carbon atoms that were added to the sulfur atoms to the two ketone oxygen atoms from an initial insertion adduct similar to that shown in Scheme 1. The infrared spectrum of **6** is similar to that of $Fe_2(CO)_6(\mu\text{-}S_2)$ except that all absorptions are shifted to lower frequencies. Details of molecular structure of **6** were established by a single-crystal X-ray diffraction analysis, and an ORTEP diagram of its molecular structure is shown in Figure 8. Selected bond distances and angles are listed in Table 5.

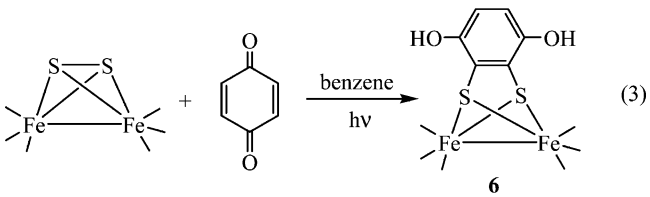


(3)

The structure of **6** is similar to that of $Fe_2(CO)_6(\mu\text{-}S_2)$ except that a hydroquinone-2,3-dithiolato ligand bridges two iron atoms instead of the disulfido ligand. The Fe−Fe bond distance, 2.4815(4) Å, is slightly shorter than that found in $Fe_2(CO)_6(\mu\text{-}S_2)$, 2.552(2) Å.[19] The S(1)···S(2) distance, 2.928

(19) Wei, C. H.; Dahl, L. F. *Inorg. Chem.* **1965**, *4*, 1.

**Table 4.** Selected Intramolecular Bond Distances and Angles for **5**[a]

(a) Distances

| atom | atom | distance (Å) | atom | atom | distance (Å) |
|---|---|---|---|---|---|
| Mo(1) | S(1) | 2.4801(6) | O(32) | C(32) | 1.354(3) |
| Mo(1) | S(2) | 2.4859(6) | O(35) | C(35) | 1.350(3) |
| Mo(1) | Mn(1) | 2.7405(4) | C(30) | C(35) | 1.383(3) |
| Mn(1) | S(2) | 2.3263(7) | C(30) | C(31) | 1.389(3) |
| Mn(1) | S(1) | 2.3354(6) | C(31) | C(32) | 1.377(3) |
| S(1) | C(30) | 1.783(2) | C(32) | C(33) | 1.397(3) |
| S(2) | C(31) | 1.787(2) | C(33) | C(34) | 1.378(3) |
| Cl(1) | C(33) | 1.722(2) | C(34) | C(35) | 1.401(3) |
| Cl(2) | C(34) | 1.725(2) | C | O | 1.140(3) (av) |
| | | | S(1) | S(2) | 2.994(3) |

(b) Angles

| atom | atom | atom | angle (deg) | atom | atom | atom | angle (deg) |
|---|---|---|---|---|---|---|---|
| S(1) | Mo(1) | S(2) | 74.158(18) | Mn(1) | S(2) | Mo(1) | 69.339(17) |
| S(1) | Mo(1) | Mn(1) | 52.860(15) | C(35) | C(30) | C(31) | 120.7(2) |
| S(2) | Mo(1) | Mn(1) | 52.584(16) | C(35) | C(30) | S(1) | 122.69(16) |
| S(2) | Mn(1) | S(1) | 79.92(2) | C(31) | C(30) | S(1) | 116.59(16) |
| S(2) | Mn(1) | Mo(1) | 58.077(16) | C(32) | C(31) | S(2) | 121.54(17) |
| S(1) | Mn(1) | Mo(1) | 57.840(16) | C(30) | C(31) | S(2) | 116.82(16) |
| C(30) | S(1) | Mn(1) | 102.64(7) | C(34) | C(33) | Cl(1) | 121.38(17) |
| C(30) | S(1) | Mo(1) | 100.35(7) | C(32) | C(33) | Cl(1) | 117.99(18) |
| Mn(1) | S(1) | Mo(1) | 69.300(17) | C(33) | C(34) | Cl(2) | 120.12(17) |
| C(31) | S(2) | Mn(1) | 102.26(7) | C(35) | C(34) | Cl(2) | 118.54(18) |
| C(31) | S(2) | Mo(1) | 100.48(7) | | | | |

[a] Estimated standard deviations in the least significant figure are given in parentheses.

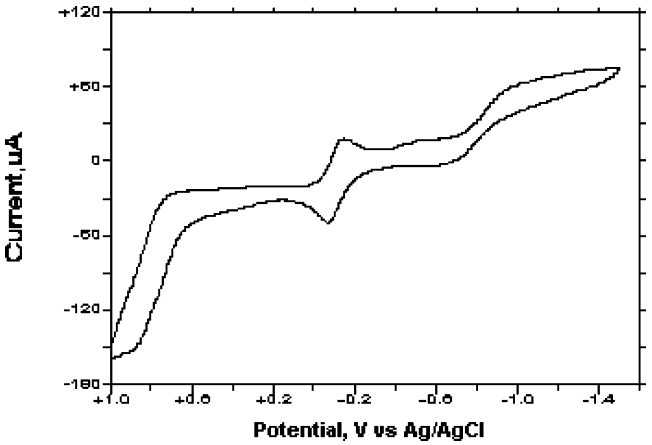


**Figure 7.** CV trace of **5** (1.0 mM) in $CH_3CN$ (10 mL) with 1.5 mM of $[NBu^n_4]OH$ and 0.1 M $[NBu^n_4]PF_6$ at scan rate 60 mV/s.

(3) Å, is nonbonding, and is longer than that found in the related compound $Fe_2(CO)_6S_2[C(Ph)=C(Ph)]$, 2.861(7) Å [2.871(7) Å].[20] The $C_6$ ring is fully delocalized, and all C−C bond distances lie in the range, 1.371(3)−1.392(3) Å. In the solid state the molecules of the complex are arranged in zigzag chains that are linked by hydrogen bonds between the hydroxyl groups of the hydroquinone functions, see Figure 9. The electrochemical properties of **6** were measured by cyclic voltammetry, and a typical CV trace is shown in Figure 10. The redox couples were observed at −0.149 V, −0.80 V versus Ag/AgCl. The redox couples are quasi-reversible.

Oxidation of compound **6** by 2,3-dichloro-5,6-dicyano-1,4-benzoquinone yielded the quinonedithiolato complex

(20) Weber, H. P.; Bryan, R. F. *J. Chem. Soc. A* **1967**, 182.

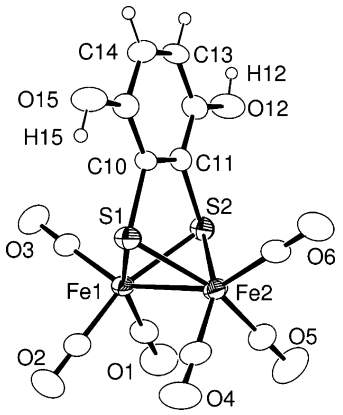


**Figure 8.** ORTEP diagram of the molecular structure of **6** showing 40% thermal ellipsoid probability.

$Fe_2(CO)_6(\mu\text{-}S_2C_6H_2O_2)$, **7**, in 87% yield, eq 4. The molecular structure of **7** was characterized by a single-crystal X-ray diffraction analysis, and an ORTEP diagram of its molecular structure is shown in Figure 11. Selected bond distances and angles are listed in Table 6.

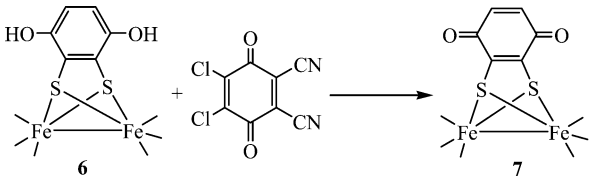


**6** **7** (4)

The Fe−Fe bond distance in **7**, 2.4687(12) Å, is shorter than that in **6**. The $C_6H_2O_2$ portion of **7** is quinone-like; the C−O distances are short, C(12)−O(12) = 1.213(7) Å and C(15)−O(15) = 1.212(7) Å and two of the ring C−C bonds are double, C(10)−C(11) = 1.334(8) Å, C(13)−C(14) =

**Table 5.** Selected Intramolecular Bond Distances and Angles for 6[a]

(a) Distances

| atom | atom | distance (Å) | atom | atom | distance (Å) |
|---|---|---|---|---|---|
| Fe(1) | S(1) | 2.2586(5) | O(15) | C(15) | 1.378(2) |
| Fe(1) | S(2) | 2.2712(5) | C(10) | C(11) | 1.392(2) |
| Fe(1) | Fe(2) | 2.4815(4) | C(10) | C(15) | 1.377(2) |
| Fe(2) | S(2) | 2.2666(5) | C(11) | C(12) | 1.376(2) |
| Fe(2) | S(1) | 2.2667(5) | C(12) | C(13) | 1.392(3) |
| S(1) | C(10) | 1.7802(17) | C(13) | C(14) | 1.371(3) |
| S(2) | C(11) | 1.7773(18) | C(14) | C(15) | 1.392(3) |
| O(12) | C(12) | 1.371(2) | C | O | 1.130(3) (av) |
| | | | S(1) | S(2) | 2.928(3) |

(b) Angles

| Atom | atom | atom | angle (deg) | atom | atom | atom | angle (deg) |
|---|---|---|---|---|---|---|---|
| S(1) | Fe(1) | S(2) | 80.525(18) | C(11) | S(2) | Fe(2) | 101.38(6) |
| S(1) | Fe(1) | Fe(2) | 56.901(15) | C(11) | S(2) | Fe(1) | 101.33(6) |
| S(2) | Fe(1) | Fe(2) | 56.759(14) | Fe(2) | S(2) | Fe(1) | 66.302(15) |
| S(2) | Fe(2) | S(1) | 80.453(18) | C(11) | C(10) | C(15) | 120.67(16) |
| S(2) | Fe(2) | Fe(1) | 56.939(15) | C(15) | C(10) | S(1) | 124.25(14) |
| S(1) | Fe(2) | Fe(1) | 56.590(14) | C(11) | C(10) | S(1) | 115.06(13) |
| C(10) | S(1) | Fe(1) | 101.49(6) | C(10) | C(11) | C(12) | 120.67(16) |
| C(10) | S(1) | Fe(2) | 102.12(6) | C(10) | C(11) | S(2) | 116.06(13) |
| Fe(1) | S(1) | Fe(2) | 66.509(16) | C(12) | C(11) | S(2) | 123.21(14) |

[a] Estimated standard deviations in the least significant figure are given in parentheses.

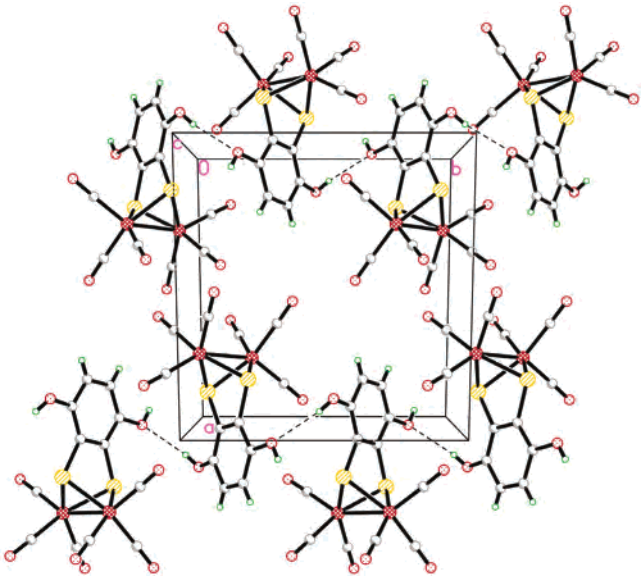

**Figure 9.** Packing diagram of the structure of **6** showing intermolecular hydrogen bonding between the hydroquinone groups.

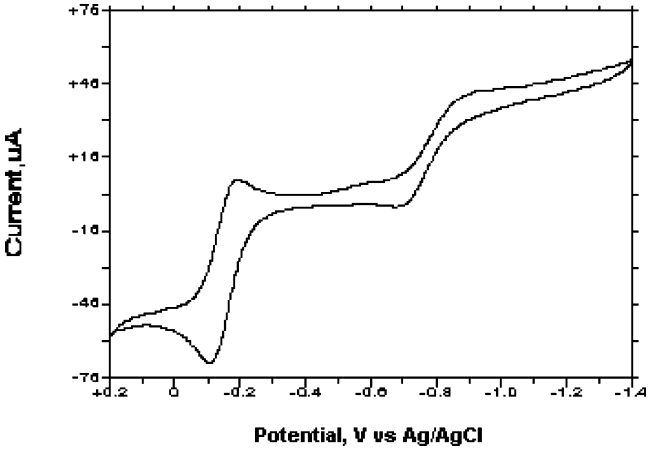


**Figure 10.** CV trace of **6** (1.5 mM) in $CH_3CN$ (10 mL) with 1.5 mM of $[Bu^n_4N]OH$ and 0.1 M $[Bu^n_4N]PF_6$ at scan rate 60 mV/s.

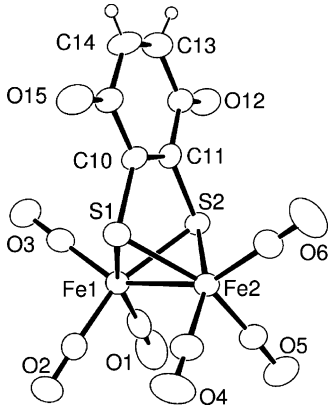


**Figure 11.** ORTEP diagram of the molecular structure of **7** showing 40% thermal ellipsoid probability.

1.304(10). The nonbonding S···S distance, 2.968 (8) Å, is slightly longer than that in **6**. Compound **7** is readily reduced to **6** as suggested by formation of **6** in the original reaction. When **7** was treated with hydrogen at room temperature in the presence of light, it was reduced to **6** in 95% yield within 12 h.

The monosubstituted $PPh_3$ derivative of **6**, $Fe_2(CO)_5(PPh_3)$-$[\mu$-$S_2C_6H_2(OH)_2]$, **8**, was obtained in 55% yield from the reaction of **6** with $PPh_3$ in the presence of a stoichiometric amount of $Me_3NO$ decarbonylation agent, Scheme 3. Compound **8** was characterized by a combination of IR, $^1H$ NMR and a single-crystal X-ray diffraction analysis. Compound **8** contains two independent molecules in the asymmetric crystal unit. Both molecules are structurally similar and an ORTEP diagram of the molecular structure of **8** is shown in Figure 12. Selected bond distances and angles are listed in Table 7. The molecular structure of **8** is similar to that of compound

**Table 6.** Selected Intramolecular Bond Distances and Angles for 7[a]

(a) Distances

| atom | atom | distance (Å) | atom | atom | distance (Å) |
|---|---|---|---|---|---|
| Fe(1) | S(2) | 2.2766(17) | O(15) | C(15) | 1.212(7) |
| Fe(1) | S(1) | 2.3000(18) | C(10) | C(11) | 1.334(8) |
| Fe(1) | Fe(2) | 2.4687(12) | C(10) | C(15) | 1.478(8) |
| Fe(2) | S(1) | 2.2742(18) | C(11) | C(12) | 1.479(8) |
| Fe(2) | S(2) | 2.2832(17) | C(12) | C(13) | 1.466(9) |
| S(1) | C(10) | 1.783(6) | C(13) | C(14) | 1.304(10) |
| S(2) | C(11) | 1.781(6) | C(14) | C(15) | 1.473(9) |
| O(12) | C(12) | 1.213(7) | C | O | 1.131(7) (av) |
| | | | S(1) | S(2) | 2.968(8) |

(b) Angles

| atom | atom | atom | angle (deg) | atom | atom | atom | angle (deg) |
|---|---|---|---|---|---|---|---|
| S(2) | Fe(1) | S(1) | 80.86(6) | C(11) | S(2) | Fe(1) | 98.93(19) |
| S(2) | Fe(1) | Fe(2) | 57.35(5) | C(11) | S(2) | Fe(2) | 101.19(18) |
| S(1) | Fe(1) | Fe(2) | 56.84(5) | Fe(1) | S(2) | Fe(2) | 65.56(5) |
| S(1) | Fe(2) | S(2) | 81.27(6) | C(11) | C(10) | C(15) | 120.8(5) |
| S(1) | Fe(2) | Fe(1) | 57.84(5) | C(11) | C(10) | S(1) | 116.8(5) |
| S(2) | Fe(2) | Fe(1) | 57.09(5) | C(15) | C(10) | S(1) | 122.4(4) |
| C(10) | S(1) | Fe(2) | 101.19(19) | C(10) | C(11) | C(12) | 122.4(5) |
| C(10) | S(1) | Fe(1) | 99.3(2) | C(10) | C(11) | S(2) | 117.8(4) |
| Fe(2) | S(1) | Fe(1) | 65.32(5) | C(12) | C(11) | S(2) | 119.7(4) |

[a] Estimated standard deviations in the least significant figure are given in parentheses.

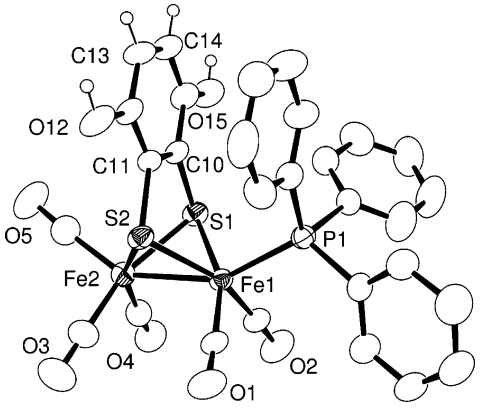


**Figure 12.** ORTEP diagram of the molecular structure of **8** showing 40% thermal ellipsoid probability.

**Scheme 3**

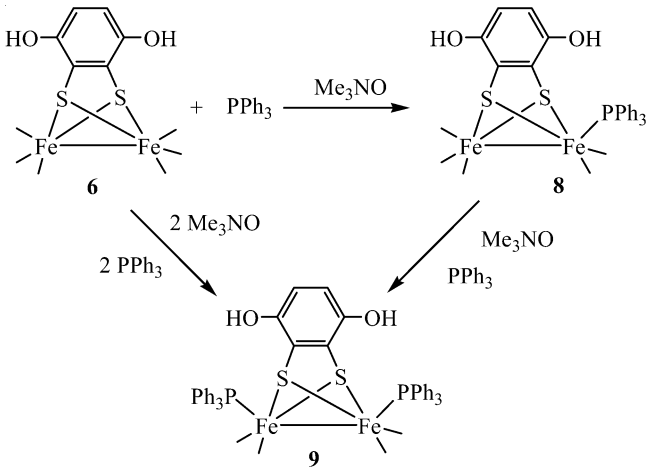


**6** except that one of the terminal CO ligands on one of the iron atoms has been replaced by a $PPh_3$ ligand. The bulky $PPh_3$ ligand prefers the less crowded axial position on the iron atom, which is consistent with the $^1H$ NMR spectrum that shows only a singlet at 5.85 ppm for the two protons on the aromatic ring. The Fe−Fe bond distance, 2.4983(12) Å [2.4991(12) Å], is longer than that in **6**, probably due to the coordination of the $PPh_3$ ligand on one of iron atoms. The Fe−P bond distance, 2.2484(18) Å [2.2524(18) Å], is similar to that observed in $Fe_2S_2(CO)_5(C_6H_3CH_3)(PPh_3)$, 2.252(2) Å.[21]

The bis-$PPh_3$ substituted derivative of **6**, $Fe_2(CO)_4(PPh_3)_2$-[$\mu$-$S_2C_6H_2(OH)_2$], **9**, was obtained from the reaction of **6** with $PPh_3$ in the presence of an excess amount of $Me_3NO$ in 56% yield, Scheme 3. $^1H$ NMR spectrum of **9** exhibits one singlet for the protons on aromatic ring at 5.48 ppm. $^{31}P$ NMR spectrum of **9** shows a single peak at 57.94 ppm. Details of the molecular structure of **9** were established by a single-crystal X-ray diffraction analysis, and an ORTEP diagram of its molecular structure is shown in Figure 13. Selected bond distances and angles are listed in Table 8. The molecular structure of **9** is also similar to that of **6** except that two CO ligands, one CO ligand on each iron atom, have been replaced by two $PPh_3$ ligands. As expected, both $PPh_3$ ligands occupy the less crowded axial positions on each iron atom. The Fe−Fe bond distance, 2.5102(6) Å, is even longer than that in **8**, but shorter than that in $Fe_2(S_2C_2(SMe)_2)(CO)_4$-$(PPh_3)_2$, 2.525(2) Å.[22] The Fe−P distances, 2.2546(9) Å and 2.2579(9) Å, are longer than those in **8**. As expected, compound **9** could be obtained from **8** by treatment with $Me_3NO$ in the presence of $PPh_3$, see Scheme 3.

The electrochemical properties of **8** and **9** were measured by cyclic voltammetry in acetonitrile solvent by using

(21) Hasan, M. M.; Hursthouse, M. B.; Kabir, S. E.; Abdul Malik, K. M. *Polyhedron* **2001**, *20*, 97.
(22) Touchard, D.; Fillaut, J.-L.; Dixneuf, P.; Mealli, C.; Sabat, M.; Toupet, L. *Organometallics* **1985**, *4*, 1684.

**Table 7.** Selected Intramolecular Bond Distances and Angles for **8**[a]

(a) Distances

| atom | atom | distance (Å) | atom | atom | distance (Å) |
|---|---|---|---|---|---|
| Fe(1) | P(1) | 2.2484(18) | Fe(3) | P(2) | 2.2524(18) |
| Fe(1) | S(2) | 2.2734(16) | Fe(3) | S(4) | 2.2716(17) |
| Fe(1) | S(1) | 2.2757(16) | Fe(3) | S(3) | 2.2758(17) |
| Fe(1) | Fe(2) | 2.4983(12) | Fe(3) | Fe(4) | 2.4991(12) |
| Fe(2) | S(1) | 2.2695(18) | Fe(4) | S(4) | 2.2667(18) |
| Fe(2) | S(2) | 2.2735(18) | Fe(4) | S(3) | 2.2825(18) |
| S(1) | C(10) | 1.771(6) | S(3) | C(50) | 1.790(6) |
| S(2) | C(11) | 1.766(5) | S(4) | C(51) | 1.777(6) |
| O(12) | C(12) | 1.356(8) | O(52) | C(52) | 1.406(8) |
| O(15) | C(15) | 1.361(8) | O(55) | C(55) | 1.375(8) |
| C(10) | C(11) | 1.384(8) | C(50) | C(55) | 1.343(9) |
| C(10) | C(15) | 1.406(9) | C(50) | C(51) | 1.416(8) |
| C(11) | C(12) | 1.402(9) | C(51) | C(52) | 1.358(9) |
| C(12) | C(13) | 1.395(9) | C(52) | C(53) | 1.396(10) |
| C(13) | C(14) | 1.393(10) | C(53) | C(54) | 1.346(11) |
| C(14) | C(15) | 1.392(10) | C(54) | C(55) | 1.421(11) |
| C | O | 1.150(9)(av) | S(1) | S(2) | 2.931(11) |
| | | | S(3) | S(4) | 2.934(11) |

(b) Angles

| atom | atom | atom | angle (deg) | atom | atom | atom | angle (deg) |
|---|---|---|---|---|---|---|---|
| P(1) | Fe(1) | S(2) | 106.13(6) | P(2) | Fe(3) | S(4) | 106.39(7) |
| P(1) | Fe(1) | S(1) | 101.72(6) | P(2) | Fe(3) | S(3) | 100.79(6) |
| S(2) | Fe(1) | S(1) | 80.23(6) | S(4) | Fe(3) | S(3) | 80.37(6) |
| P(1) | Fe(1) | Fe(2) | 152.13(6) | P(2) | Fe(3) | Fe(4) | 151.72(6) |
| S(2) | Fe(1) | Fe(2) | 56.67(5) | S(4) | Fe(3) | Fe(4) | 56.49(5) |
| S(1) | Fe(1) | Fe(2) | 56.54(5) | S(3) | Fe(3) | Fe(4) | 56.88(5) |
| S(1) | Fe(2) | S(2) | 80.36(6) | S(4) | Fe(4) | S(3) | 80.33(6) |
| S(1) | Fe(2) | Fe(1) | 56.78(5) | S(4) | Fe(4) | Fe(3) | 56.68(5) |
| S(2) | Fe(2) | Fe(1) | 56.67(5) | S(3) | Fe(4) | Fe(3) | 56.62(5) |
| C(10) | S(1) | Fe(2) | 100.4(2) | C(50) | S(3) | Fe(3) | 102.66(18) |
| C(10) | S(1) | Fe(1) | 102.09(19) | C(50) | S(3) | Fe(4) | 100.4(2) |
| Fe(2) | S(1) | Fe(1) | 66.69(5) | Fe(3) | S(3) | Fe(4) | 66.49(5) |
| C(11) | S(2) | Fe(1) | 102.65(19) | C(51) | S(4) | Fe(4) | 100.6(2) |
| C(11) | S(2) | Fe(2) | 100.0(2) | C(51) | S(4) | Fe(3) | 103.7(2) |
| Fe(1) | S(2) | Fe(2) | 66.66(5) | Fe(4) | S(4) | Fe(3) | 66.83(5) |

[a] Estimated standard deviations in the least significant figure are given in parentheses.

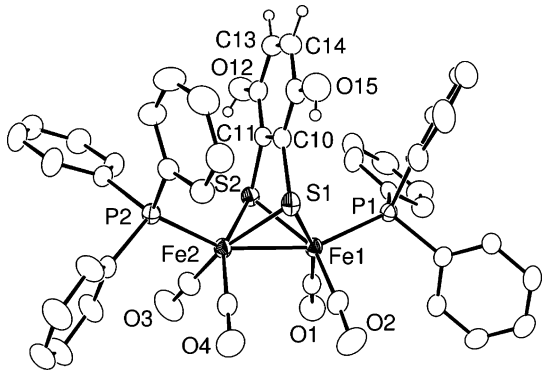


**Figure 13.** ORTEP diagram of the molecular structure of **9** showing 40% thermal ellipsoid probability.

tetrabutylammonium hexafluorophosphate as the supporting electrolyte. CV traces of **8** and **9** are shown in Figures 14 and 15, respectively. The redox couples for **8** and **9** were observed at −0.289 −1.10 V and −0.449, −1.20 V versus Ag/AgCl, respectively. These redox couples are quasi-reversible. The more negative potentials for **8** and **9** compared to **6** can be attributed to effects from the $PPh_3$ ligands which are better electron donors to the metal atoms, i.e., they add more electron density to the complex which in turn makes it more difficult to put additional electrons onto the complex electrochemically.

Like that addition of olefins to **1**, all quinone additions to **1** and $Fe_2(CO)_6(\mu\text{-}S_2)$ require irradiation. Interestingly, the quinone addition to $Fe_2(CO)_6(\mu\text{-}S_2)$ requires UV irradiation and does not occur under similar conditions by using irradiation from a tungsten source. The quinone additions to **1** proceed with irradiation with visible light. This difference in frequencies suggests that it is the metal complex that requires the activation by irradiation and not the quinone molecule which is the same (1,4-benzoquinone) for both reactions and also that the activation process for $Fe_2(CO)_6(\mu\text{-}S_2)$ occurs at higher energy than that for **1**. Accordingly, we recorded the UV−vis absorption spectra of $Fe_2(CO)_6(\mu\text{-}S_2)$, **1**, **2**, **3**, **6**, and **7** in toluene solvent. The absorptions and their extinction coefficients are listed in Table 9. Indeed, the absorptions of **1** do occur at longer wavelengths, 342 and 403 nm than that in $Fe_2(CO)_6(\mu\text{-}S_2)$, 338 nm. Interestingly, the absorptions of the benzoquinone derivatives **2** (338 nm) and **7** (325 nm) lie at shorter wavelengths than those of their corresponding hydroquinone forms **3** (351 nm) and **6** (331 and 398 nm). This indicates that the more reducing hydroquinone group is able to lower the energy of the transitions

**Table 8.** Selected Intramolecular Bond Distances and Angles for **9**[a]

(a) Distances

| atom | atom | distance (Å) | atom | atom | distance (Å) |
|---|---|---|---|---|---|
| Fe(1) | P(1) | 2.2546(9) | O(12) | C(12) | 1.366(4) |
| Fe(1) | S(2) | 2.2888(8) | O(15) | C(15) | 1.368(4) |
| Fe(1) | S(1) | 2.2914(9) | C(10) | C(11) | 1.399(4) |
| Fe(1) | Fe(2) | 2.5102(6) | C(10) | C(15) | 1.377(4) |
| Fe(2) | P(2) | 2.2579(9) | C(11) | C(12) | 1.377(4) |
| Fe(2) | S(2) | 2.2867(8) | C(12) | C(13) | 1.387(5) |
| Fe(2) | S(1) | 2.2878(9) | C(13) | C(14) | 1.362(5) |
| S(1) | C(10) | 1.797(3) | C(14) | C(15) | 1.391(5) |
| S(2) | C(11) | 1.784(3) | C | O | 1.144(4) (av) |
| | | | S(1) | S(2) | 2.931(5) |

(b) Angles

| atom | atom | atom | angle (deg) | atom | atom | atom | angle (deg) |
|---|---|---|---|---|---|---|---|
| P(1) | Fe(1) | S(2) | 108.66(3) | C(10) | S(1) | Fe(2) | 102.45(11) |
| P(1) | Fe(1) | S(1) | 103.69(3) | C(10) | S(1) | Fe(1) | 101.45(10) |
| S(2) | Fe(1) | S(1) | 79.57(3) | Fe(2) | S(1) | Fe(1) | 66.48(3) |
| P(1) | Fe(1) | Fe(2) | 155.40(3) | C(11) | S(2) | Fe(2) | 103.22(10) |
| S(2) | Fe(1) | Fe(2) | 56.69(2) | C(11) | S(2) | Fe(1) | 101.85(10) |
| S(1) | Fe(1) | Fe(2) | 56.69(2) | Fe(2) | S(2) | Fe(1) | 66.54(2) |
| P(2) | Fe(2) | S(2) | 112.25(3) | C(15) | C(10) | C(11) | 120.0(3) |
| P(2) | Fe(2) | S(1) | 99.91(3) | C(15) | C(10) | S(1) | 124.4(3) |
| S(2) | Fe(2) | S(1) | 79.69(3) | C(11) | C(10) | S(1) | 115.5(2) |
| P(2) | Fe(2) | Fe(1) | 154.21(3) | C(12) | C(11) | C(10) | 120.5(3) |
| S(2) | Fe(2) | Fe(1) | 56.77(2) | C(12) | C(11) | S(2) | 124.3(3) |
| S(1) | Fe(2) | Fe(1) | 56.83(2) | C(10) | C(11) | S(2) | 115.1(2) |

[a] Estimated standard deviations in the least significant figure are given in parentheses.

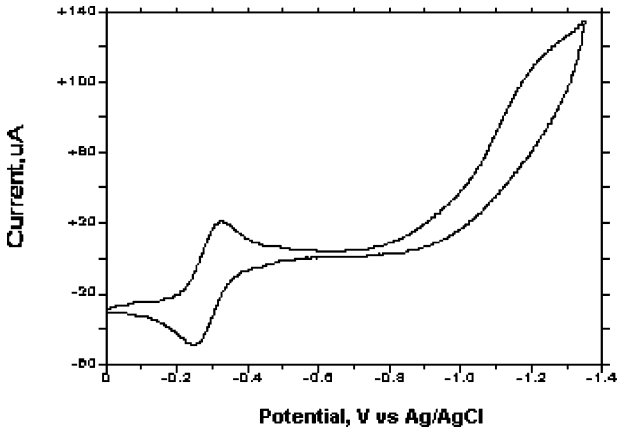


**Figure 14.** CV trace of **8** (1.5 mM) in $CH_3CN$ (10 mL) with 1.5 mM of $[NBu^n_4]OH$ and 0.1 M $[Bu^n_4N]PF_6$ at scan rate 100 mV/s.

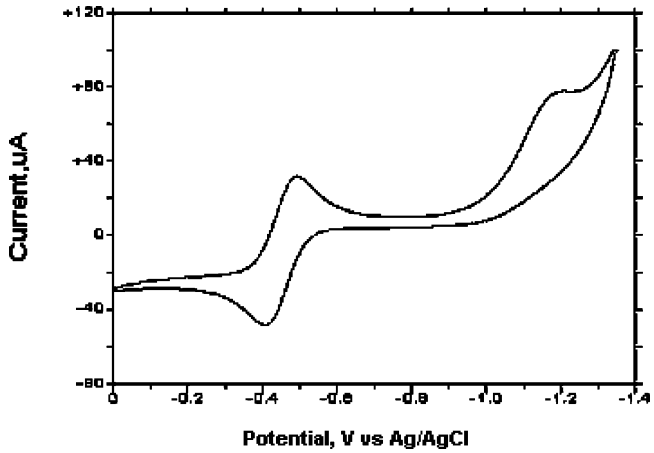


**Figure 15.** CV trace of **9** (1.5 mM) in $CH_3CN$ (10 mL) with 1.5 mM of $[Bu^n_4N]OH$ and 0.1 M of $[Bu^n_4N]PF_6$ at scan rate 100 mV/s.

in the metal complexes slightly compared to that of the more oxidizing quinone group.

The redox chemistry of quinones is complex but well understood.[23]

Reductions involve a series of two, one-electron transfers coupled with proton additions culminating with the formation of the hydroquinones. The cyclic voltammograms of **3**−**9** are consistent with the established redox properties of quinones. These results are summarized in Table 10. All of compounds show a one electron redox event in the range −0.45− −0.11 V vs Ag/AgCl. This is assigned to the quinone to quinone$^{-1}$ redox couple. A second redox couple that lies in the range −0.80− −1.20 V vs Ag/AgCl is of poor quality and is irreversible, probably due to the involvement of protonation steps. It can be attributed to quinone$^{-1}$ to qunione$^{-2}$ redox event. These are similar to those observed for free quinones, but occur at more negative potentials due

**Table 9.** UV−Vis Absorption Data for $Fe_2(CO)_6(\mu\text{-}S_2)$, **1**, **2**, **3**, **6**, and **7**[a]

| compd | $\lambda_{max}$ (nm) (absorption coefficient ($\epsilon$, $M^{-1}$ $cm^{-1}$)) |
|---|---|
| $Fe_2(CO)_6(\mu\text{-}S_2)$ | 338 (15594) |
| **1** | 342 (5465), 403 (2530) |
| **2** | 338 (5666) |
| **3** | 351 (6334) |
| **6** | 331 (9978), 398 (4421) |
| **7** | 325 (2921) |

[a] Recorded in toluene solvent.

(23) (a) Eggins, B. R. *Chem. Commun.* **1969**, 1267. (b) Parker, V. D. *Chem. Commun.* **1969**, 716. (c) Sembiring, S. B.; Colbran, S. B.; Craig, D. C. *J. Chem. Soc., Dalton Trans.* **1999**, 1543. (d) Storrier, G. D.; Colbran, S. B.; Craig, D. C. *J. Chem. Soc., Dalton Trans.* **1998**, 1351.

**Table 10.** Electrochemical Data for **3**, **5**, **6**, **8**, and **9**[a]

| compd | first redox wave | second redox wave |
|---|---|---|
| **3** | −0.34 | −1.0 |
| **5** | −0.11 | −0.9 |
| **6** | −0.149 | −0.80 |
| **8** | −0.289 | −1.10 |
| **9** | −0.449 | −1.20 |

[a] $E_{1/2}$ (V) vs Ag/AgCl.

to the electron donating properties of the metal groupings to the quinone rings. The redox potentials of **5** are more positive than those of **3** because two chlorine atoms on the quinone ring are more electron withdrawing than the hydrogen atoms on **3**. The potentials of **8** and **9** are more negative than **6** because the phosphine ligands are more electron donating than the CO ligands on **6** that they replaced.

To summarize, we have now synthesized the first mixed-metal benzoquinonedithiolate compounds, **2** and **4**, by reactions of **1** with the appropriate benzoquinones under irradiation with visible light. 1,4-Benzoquinone and 2, 3-dichloro-1,4-benzoquinone were inserted into S−S bond of $CpMoMn(CO)_5(\mu\text{-}S_2)$ to form **2** and **4**, respectively. Compounds **2** and **4** were reduced by hydrogen to provide the hydroquinone derivatives **3** and **5**. $Fe_2(CO)_6(\mu\text{-}S_2)$ also reacts with quinones, but the product obtained was the hydroquinone complex **6**. Compound **6** however, could be oxidized to the quinone complex **7** which was also isolated and structurally characterized.

## Experimental Section

**General Data.** All reactions were performed under a nitrogen atmosphere using Schlenk techniques. Reagent grade solvents were dried by the standard procedures and were freshly distilled prior to use. Infrared spectra were recorded on a Thermo-Nicolet Avatar 360 FTIR spectrophotometer. $^1$H NMR spectra were recorded on a Varian Inova 300 spectrometer operating at 300 MHz. $^{31}$P NMR spectra were recorded on a Varian Inova 400 spectrometer operating at 161.955 MHz. Elemental analyses were performed by Desert Analytics (Tucson, AZ). Mass spectra were recorded on a VG70SQ mass spectrometer. UV−vis absorption spectra were measured in toluene solutions by using a JASCO V-530 UV/visible spectrophotometer. 1,4-Benzoquinone, 2,3-dichloro-1,4-benzoquinone, ferrocenium hexafluorophosphate, 2,3-dichloro-5,6-dicyano-1,4-benzoquinone were purchased from Aldrich Co. $PPh_3$ was obtained from Columbia Organic Chemicals Co. Inc. and was used without further purification. $Me_3NO{\cdot}2H_2O$ was purchased from Aldrich Co. and dehydrated before use. $CpMoMn(CO)_5(\mu\text{-}S_2)$[4] and $Fe_2(CO)_6(\mu\text{-}S_2)$[24] were prepared according to the published procedures. All product separations were performed by TLC in air on Analtech 0.25 and 0.5 mm silica gel 60 Å $F_{254}$ glass plates.

**Synthesis of $CpMoMn(CO)_5(\mu\text{-}S_2C_6H_2O_2)$, 2.** 1,4-Benzoquinone (62 mg, 0.57 mmol) was added to a solution of $CpMoMn(CO)_5(\mu\text{-}S_2)$ (30 mg, 0.071 mmol) in benzene (40 mL). The solution was stirred at room temperature for 24 h in the presence of irradiation from a 150 W tungsten lamp (12 in.). The solvent was then removed in vacuo and the residue was separated by TLC by using $CH_2Cl_2$ solvent as eluant. A total of 25 mg of $CpMoMn(CO)_5(\mu\text{-}S_2C_6H_2O_2)$, **2** (67% yield), was obtained. Spectral data for **2**: IR $\nu_{CO}$ ($cm^{-1}$ in $CH_2Cl_2$) 2035(vs), 1994(m), 1959(m), 1931-(m), 1651(m). $^1$H NMR ($\delta$ in $CDCl_3$) 6.62 (s, 2H), 5.98 (s, 5H). $^{13}$C NMR ($\delta$ in $CD_2Cl_2$) 235.22, 180.88, 169.07, 136.70, 96.27. MS (ES) *m*/*z* 528 ($M^+$). Anal. Calc. for $C_{16}H_7MnMoO_7S_2$: C(%), 36.52; H(%), 1.34. Found C, 36.44; H, 1.50.

**Reduction of 2 to $CpMoMn(CO)_5[\mu\text{-}S_2C_6H_2(OH)_2]$, 3, by Hydrogen.** A solution of **2** (15 mg, 0.028 mmol) in $CH_2Cl_2$ (30 mL) was purged with hydrogen for 10 min. The solution was stirred at room temperature under a hydrogen atmosphere in room light for 12 h. The solvent was removed in vacuo and the residue was separated by TLC by using $CH_2Cl_2$ solvent as eluant. A total of 13 mg of $CpMoMn(CO)_5[\mu\text{-}S_2C_6H_2(OH)_2]$, **3** (85% yield), was obtained. Spectral data for **3**: IR $\nu_{CO}$ ($cm^{-1}$ in $CH_2Cl_2$) 2030(vs), 1989(m), 1954(m), 1923(m). $^1$H NMR ($\delta$ in $CDCl_3$) 6.22 (s, 2H), 5.68 (s, 5H), 4.82 (s, 2H). $^{13}$C NMR ($\delta$ in $CD_2Cl_2$) 235.12, 148.94, 133.85, 116.34, 95.82. MS (ES) *m*/*z* 530 ($M^+$). Anal. Calc. for $C_{16}H_9MnMoO_7S_2{\cdot}O(C_2H_5)_2$: C(%), 39.88; H(%), 3.18. Found C, 40.42; H, 3.49.

**Oxidation of 3 to 2.** Ferrocenium hexafluorophosphate (47 mg, 0.14 mmol) was added to a solution of **3** (15 mg, 0.028 mmol) in $CH_2Cl_2$ (30 mL). The solution was stirred at room temperature for 12 h. The solvent was then removed in vacuo and the residue was separated by TLC by using $CH_2Cl_2$ solvent for elution. A total of 12.5 mg of $CpMoMn(CO)_5(\mu\text{-}S_2C_6H_2O_2)$, **2** (84% yield), was obtained.

**Synthesis of $CpMoMn(CO)_5(\mu\text{-}S_2C_6Cl_2O_2)$, 4.** 2,3-Dichloro-1,4-benzoquinone (19 mg, 0.11 mmol) was added to a solution of **1** (15 mg, 0.0357 mmol) in benzene (30 mL). The solution was stirred at room temperature for 12 h in the presence of irradiation from a 150 W tungsten lamp (12 in. from the flask). The solvent was then removed in vacuo and the residue was separated by TLC using hexane/$CH_2Cl_2$ (1/1, v/v) solvent mixture as eluant. A total of 8.0 mg of **4** (38% yield) was obtained. Spectral data for **4**: IR $\nu_{CO}$ ($cm^{-1}$ in $CH_2Cl_2$) 2037(vs), 1996(m), 1961(m), 1934(m), 1668(m). $^1$H NMR ($\delta$ in $CDCl_3$) 6.025 (s, 5H). Anal. Calc. for $C_{16}H_5MnMoO_7S_2Cl_2{\cdot}CH_2Cl_2$: C(%), 30.02; H(%), 1.04. Found C, 30.55; H, 1.22.

**Reduction of 4 to $CpMoMn(CO)_5[\mu\text{-}S_2C_6Cl_2(OH)_2]$, 5, by Hydrogen.** A solution of **4** (15 mg, 0.025 mmol) in benzene was stirred at room temperature under a hydrogen atmosphere in the presence of room light for 12 h. The solvent was removed in vacuo and the residue was separated by TLC using $CH_2Cl_2$ solvent as eluant. A total of 12.5 mg of $CpMoMn(CO)_5[\mu\text{-}S_2C_6Cl_2(OH)_2]$, **5** (83% yield), was obtained. Spectral data for **5**: IR $\nu_{CO}$ ($cm^{-1}$ in $CH_2Cl_2$) 2031(vs), 1990(m), 1956(m), 1923(m). $^1$H NMR ($\delta$ in $CDCl_3$) 5.73 (s, 5H), 5.41 (s, 2H). Anal. Calc. for $C_{16}H_7Cl_2MnMoO_7S_2$: C(%), 32.18; H(%), 1.18. Found C, 32.27; H, 1.47.

**Oxidation of 5 to 4.** To a solution of **5** (15 mg, 0.025 mmol) in $CH_2Cl_2$ was added 2,3-dichloro-5,6-dicyano-1,4-benzoquinone (18 mg, 0.079 mmol). Then the solution was stirred at room temperature for 2 h. The solvent was removed in vacuo and the residue was separated by TLC using hexane/$CH_2Cl_2$ (1/1, v/v) solvent mixture as eluant to yield 12 mg of **4** (80%).

**Synthesis of $Fe_2(CO)_6[\mu\text{-}S_2C_6H_2(OH)_2]$, 6.** A 100 mg (0.291 mmol) amount of $Fe_2(CO)_6(\mu\text{-}S_2)$ was dissolved in 100 mL benzene in a 200 mL rb flask. The solution was purged with nitrogen for 20 min. To this solution was added 95 mg (0.88 mmol) of 1,4-benzoquinone. The resulting solution was irradiated for 2.5 h at room temperature by placing a 125 WPI UV-lamp 12 in. from the flask. The volatiles were removed in vacuo and the residue was separated by column over silica gel by using $CH_2Cl_2$ solvent as eluant. A total of 70 mg of **6** (53% yield) was obtained. Similar yields were also obtained when the reaction was performed in the

(24) Brandt, P. F.; Lesch, D. A.; Stafford, P. R.; Rauchfuss, T. B.; Kolis, J. W.; Roof, L. C. *Inorg. Synth.* **1997**, *31*, 112.

**Table 11.** Crystallographic Data for Compounds **2**−**9**

| param | **2** | **3** | **4** | **5** |
|---|---|---|---|---|
| empirical formula | $C_{16}H_7MnMoO_7S_2$ | $C_{16}H_9MnMoO_7S_2{\cdot}O(C_2H_5)_2$ | $C_{16}H_5Cl_2MnMoO_7S_2{\cdot}CH_2Cl_2$ | $C_{16}H_7Cl_2MnMoO_7S_2{\cdot}O(C_2H_5)_2$ |
| formula weight | 526.22 | 602.35 | 680.03 | 671.24 |
| crystal system | orthorhombic | monoclinic | orthorhombic | monoclinic |
| space group | *Pbca* | $P2_1/c$ | $Pna2_1$ | $P2_1/c$ |
| *a* (Å) | 13.1057(7) | 8.7934(4) | 16.9605(7) | 9.5384(4) |
| *b* (Å) | 16.3648(8) | 21.9625(9) | 11.0807(4) | 14.5266(6) |
| *c* (Å) | 16.8605(8) | 12.7233(6) | 24.0844(9) | 17.6895(7) |
| α (deg) | 90 | 90 | 90 | 90 |
| *β* (deg) | 90 | 97.4970(10) | 90 | 91.3470(10) |
| *γ* (deg) | 90 | 90 | 90 | 90 |
| *V* (Å$^3$) | 3616.1(3) | 2436.18(19) | 4526.3(3) | 2450.39(17) |
| *Z* | 8 | 4 | 4 | 4 |
| temperature (K) | 296(2) | 296(2) | 296(2) | 296(2) |
| $\rho_{calc}$ (g/cm$^3$) | 1.933 | 1.642 | 0.998 | 1.819 |
| $\mu$ (Mo Kα) (mm$^{-1}$) | 1.659 | 1.246 | 0.903 | 1.459 |
| no. observations ($I > 2\sigma(I)$) | 3772 | 5353 | 9667 | 5103 |
| no. parameters | 272 | 327 | 617 | 375 |
| goodness of fit[a] | 0.952 | 1.025 | 1.018 | 1.038 |
| max shift in final cycle | 0.000 | 0.001 | 0.001 | 0.005 |
| residuals: R1, wR2[b] | 0.0394, 0.1017 | 0.0267, 0.0637 | 0.0335; 0.0723 | 0.0309; 0.0701 |
| absorption corrn, max/min | SADABS, 1.000/0.847 | SADABS, 1.000/0.817 | SADABS, 1.000/0.832 | SADABS, 1.000/0.925 |
| largest peak in diff map (e$^-$/Å$^3$) | 0.740 | 0.605 | 0.692 | 0.538 |

| param | **6** | **7** | **8** | **9** |
|---|---|---|---|---|
| empirical formula | $C_{12}H_4Fe_2O_8S_2$ | $C_{12}H_2Fe_2O_8S_2$ | $C_{29}H_{19}Fe_2O_7PS_2{\cdot}O(C_2H_5)_2$ | $C_{46}H_{34}Fe_2O_6P_2S_2{\cdot}H_2O$ |
| formula weight | 451.97 | 449.96 | 760.35 | 938.51 |
| crystal system | monoclinic | monoclinic | tetragonal | triclinic |
| space group | $P2_1/c$ | $P2_1/c$ | $P4_1$ | $P\bar{1}$ |
| *a* (Å) | 11.8389(9) | 17.4569(1) | 14.0285(3) | 9.4928(3) |
| *b* (Å) | 10.8791(8) | 6.3853(4) | 14.0285(3) | 12.9430(5) |
| *c* (Å) | 12.8949(10) | 15.5109(5) | 38.4236(7) | 18.3092(9) |
| α (deg) | 90 | 90 | 90 | 110.392(2) |
| *β* (deg) | 107.068(2) | 114.1030(10) | 90 | 95.320(3) |
| *γ* (deg) | 90 | 90 | 90 | 93.468(3) |
| *V* (Å$^3$) | 1587.7(2) | 1578.22(11) | 7561.7(3) | 2089.10(15) |
| *Z* | 4 | 4 | 8 | 2 |
| temperature (K) | 296(2) | 296(2) | 296(2) | 296(2) |
| $\rho_{calc}$ (g/cm$^3$) | 1.891 | 1.894 | 1.336 | 1.492 |
| $\mu$ (Mo Kα) (mm$^{-1}$) | 2.128 | 2.140 | 0.964 | 0.923 |
| no. observations ($I > 2\sigma(I)$) | 3492 | 2292 | 10684 | 6991 |
| no. parameters | 233 | 225 | 776 | 676 |
| goodness of fit[a] | 1.051 | 1.005 | 1.055 | 1.047 |
| max shift in final cycle | 0.001 | 0.000 | 0.001 | 0.001 |
| residuals: R1, wR2[b] | 0.0293; 0.0696 | 0.0638; 0.1291 | 0.0548; 0.1559 | 0.0506; 0.1039 |
| absorption corrn, max/min | SADABS, 1.000/0.863 | SADABS, 1.000/0.859 | SADABS, 1.000/0.821 | SADABS, 1.000/0.913 |
| largest peak in diff map (e$^-$/Å$^3$) | 0.439 | 0.549 | 0.852 | 0.552 |

[a] GOF = $[\Sigma_{hkl}(w(|F_{obs}^2| - |F_{calc}^2|))^2/(n_{data} - n_{vari})]^{1/2}$. [b] $R_1 = \Sigma(||F_{obs}| - |F_{calc}||)/\Sigma F_{obs}|$. $wR_2 = \{\Sigma[w(|F_{obs}^2 - F_{calc}^2|)^2/\Sigma[w(F_{obs}^2)^2]\}^{1/2}$; $w = 1/\sigma^2(F_{obs}^2)$.

solvents: toluene, thf, $CH_2Cl_2$ and acetone. Spectral data for **6**: IR $\nu_{CO}$ (cm$^{-1}$ in hexane). 2082 (m), 2049(vs), 2012 (s), 2009 (s). $^1$H NMR ($\delta$ in $CDCl_3$), 6.22(s, 2H); 4.78(s,2H). Anal. Calc. for $C_{12}H_4Fe_2O_8S_2$: C(%), 31.89; H(%), 0.89; Found C, 31.80; H, 0.89.

**Oxidation of 6 to $Fe_2(CO)_6(\mu$-$S_2C_6H_2O_2)$, 7.** To a solution of **6** (20 mg, 0.044 mmol) in $CH_2Cl_2$ (30 mL) was added 35 mg of 2,3-dichloro-5,6-dicyano-1,4-benzoquinone. The solution was then stirred at room temperature for 12 h. The solvent was removed in vacuo and the residue was separated by TLC by using hexane/$CH_2Cl_2$ (1/1, v/v) solvent mixture as eluant. A total of 17 mg of **7** (87% yield) was obtained. Spectral data for **7**: IR $\nu_{CO}$ (cm$^{-1}$ in hexane) 2086(m), 2051(vs), 2015(vs), 1669(w). $^1$H NMR ($\delta$ in $CDCl_3$) 6.58 (s, 2H). Anal. Calc. for $C_{12}H_2Fe_2O_8S_2$: C(%), 32.03; H(%), 0.45. Found C, 31.77; H, 0.54.

**Reduction of 7 to 6.** The solution of **7** (8.0 mg, 0.018 mmol) in benzene (15 mL) was stirred at room temperature under a hydrogen atmosphere in the presence of room light for 12 h. The solvent was then removed in vacuo and the residue was separated by TLC using $CH_2Cl_2$ solvent as eluant. A total of 7.6 mg of $Fe_2(CO)_6[\mu$-$S_2C_6H_2(OH)_2]$, **6** (95% yield), was obtained.

**Synthesis of $Fe_2(CO)_5(PPh_3)[\mu$-$S_2C_6H_2(OH)_2]$, 8.** $Me_3NO$ (3.0 mg, 0.040 mmol) was added to a solution of **6** (20 mg, 0.044 mmol) and $PPh_3$ (58 mg, 0.22 mmol) in THF (20 mL). The solution was stirred at room temperature for 12 h. The solvent was then removed in vacuo and the residue was separated by TLC using hexane/$CH_2Cl_2$ (1:2, v/v) solvent mixture as eluant. A total of 17 mg of **8** (55% yield) was obtained. Spectral data for **8**: IR $\nu_{CO}$ (cm$^{-1}$ in hexane) 2057(vs), 2002(vs), 1989(s), 1949(w). $^1$H NMR ($\delta$ in $CDCl_3$) 7.54−7.47 (m, 6H), 7.42−7.37 (m, 9H), 5.85(s, 2H), 4.40(s, 2H). $^{31}$P

NMR ($\delta$ in $CDCl_3$) 61.18. Anal. Calc. for $C_{29}H_{19}Fe_2O_7PS_2$: C(%), 50.75; H(%), 2.79. Found C, 51.15; H, 2.91.

**Synthesis of $Fe_2(CO)_4(PPh_3)_2[\mu$-$S_2C_6H_2(OH)_2]$, 9.** $Me_3NO$ (7.0 mg, 0.093 mmol) was added to a solution of **6** (8.0 mg, 0.0177 mmol) and $PPh_3$ (24 mg, 0.092) in THF solvent (20 mL). The solution was stirred at room temperature for 12 h. The solvent was then removed in vacuo and the residue was separated by TLC by using a hexane/$CH_2Cl_2$ (1:1, v/v) solvent mixture as eluant. A total of 9.2 mg of **9** (56% yield) was obtained. Spectral data for **9**: IR $\nu_{CO}$ ($cm^{-1}$ in hexane) 2009(vs), 1966(m), 1952(m). $^1H$ NMR ($\delta$ in $CDCl_3$) 7.49−7.44 (m, 12H), 7.37−7.29 (m, 18H), 5.48(s, 2H), 4.00(s, 2H). $^{31}P$ NMR ($\delta$ in $CDCl_3$) 57.94. Anal. Calc. for $C_{46}H_{34}Fe_2O_6P_2S_2 \cdot H_2O$: C(%), 58.87; H(%), 3.87. Found C, 58.49; H, 3.92.

**Formation of 9 from 8.** To the solution of **8** (20 mg, 0.029 mmol) and $PPh_3$ (16 mg, 0.061 mmol) in THF (20 mL) was added $Me_3NO$ (4.0 mg, 0.053 mmol) at 0 °C. The solution was stirred at 0 °C for 12 h. The workup gave 10 mg (37% yield) of **9**.

**Electrochemical Measurements.** Cyclic voltammetric experiments were conducted by using a CV-50W voltammetric analyzer purchased from Bioanalytical Systems, West Lafayette, IN. The experiments were done under a nitrogen atmosphere at room temperature in 10 mL of $CH_3CN$ solution by using 1.0 mM solutions of compounds **3**, **5**, **6**, **8**, or **9** with 1.5 mM of $Bu^n_4NOH$ with 0.1 mol/L tetrabutylammonium hexafluorophosphate as the supporting electrolyte. Cyclic voltammograms (CVs) were obtained by using a three-electrode system consisting of a platinum working electrode, a platinum counter and an Ag/AgCl reference electrode. Half-wave potentials ($E_{1/2}$) were calculated as the mean potential between the peak potential by use of the equation $E_{1/2} = (E_{pa} + E_{pc})/2$, where $E_{pa}$ is the anodic peak potential and $E_{pc}$ is the cathodic peak potential.

**Crystallographic Analyses.** Green single crystals of compounds **2** and **4**, brown single crystals of **7**, and red single crystals of **9** were grown by slow evaporation of solvent from solutions of the complex in hexane/methylene chloride solvent mixtures at 4 °C. Orange single crystals of **6** suitable for diffraction analysis were grown by slow evaporation of solvent from a toluene solution at 4 °C. Orange single crystals of **3** and red single crystals of **5** and **8** suitable for diffraction analysis were grown by slow evaporation of solvent from solutions in ethyl ether solvent at −20 °C. The data crystal of each compound was mounted by gluing onto the end of a thin glass fiber. X-ray intensity data were measured by using a Bruker SMART APEX CCD-based diffractometer by using Mo K$\alpha$ radiation ($\lambda = 0.71073$ Å). All unit cells were initially determined based on reflections selected from a set of three scans measured in orthogonal wedges of reciprocal space. The raw data frames were integrated with the SAINT+ program using a narrow-frame integration algorithm.[25] Corrections for the Lorentz and polarization effects were also applied by using the program SAINT. An empirical absorption correction based on the multiple measurement of equivalent reflections was applied for each analysis by using the program SADABS. Crystal data, data collection parameters, and results of the analyses for compounds **2**−**9** are listed in Table 11. All structures were solved by a combination of direct methods and difference Fourier syntheses. All nonhydrogen atoms were refined with anisotropic thermal parameters. Refinements were carried out on $F^2$ by the method of full-matrix least squares by using the SHELXTL program library with neutral atom scattering factors.[26]

Compound **2** crystallized in the orthorhombic crystal system. The space group *Pbca* was identified uniquely on the basis of the systematic absences observed in the data.

Compounds **3**, **5**, **6**, and **7** crystallized in the monoclinic crystal system. The space group $P2_1/c$ was identified uniquely on the basis of the systematic absences observed in the data. One molecule of ethyl ether was found cocrystallized in the lattice of compounds **3** and **5**. It was included in the both calculations and was satisfactorily refined.

Compound **4** crystallized in the orthorhombic crystal system. The systematic absences in the data were consistent with either of the space groups $Pna2_1$ or *Pnma*. The noncentric space group $Pna2_1$ was selected and confirmed by the successful solution and refinement of the structure. Compound **4** contains two independent molecules in the asymmetric crystal unit. One equivalent of $CH_2Cl_2$ from the crystallization solvent was found cocrystallized with the complex. It was included in the calculations and was satisfactorily refined.

Compound **8** crystallized in the tetragonal crystal system. The systematic absences in the data were consistent with space groups $P4_1$ or $P4_3$. The chiral space group $P4_1$ was tested first and confirmed by the successful solution and refinement of the structure. Compound **8** contains two independent molecules in the asymmetric crystal unit. One equivalent of diethyl ether from crystallization solvent was found cocrystallized with the compound. The Flack parameter for refinement in the space group $P4_1$ was 0.0577. The Flack parameter for refinement in the space group $P4_3$ was very close to 1.0, suggesting that the correct space group was the initially chosen one $P4_1$.

Compound **9** crystallized in the triclinic crystal system. The centrosymmetric space group $P\bar{1}$ was assumed and confirmed by the successful solution and refinement of the structure. One equivalent of water was found in the lattice cocrystallized with compound **9**. It was included in the calculations and was satisfactorily refined.

**Acknowledgment.** This research was supported by a grant from the National Science Foundation, Grant CHE0354892.

**Supporting Information Available:** CIF tables for the structural analyses of compounds **2**−**9**. This material is available free of charge via the Internet at http://pubs.acs.org.

IC048880W

(25) *SAINT+, version; 6.02a*; Bruker Analytical X-ray Systems, Inc.: Madison; WI, 1998.

(26) Sheldrick, G. M. *SHELXTL, version 5.1*; Bruker Analytical X-ray Systems, Inc.: Madison, WI, 1997.